Robust Control of an Inverted Pendulum

Christopher Mayhew
Department of Electrical and Computer Engineering
University of California, Santa Barbara
Santa Barbara, 93106-9560
Email: mayhew@engineering.ucsb.edu

***Abstract*— In this paper, we consider the design of a robust controller for the Quanser inverted pendulum system. Using a randomization of uncertain parameters, a suitable perturbation model is found for the system. An $\mathcal{H}_\infty$ design is employed to control the nomial model and a μ test is used to analyze its robust performance. D-K iteration is then performed on the $\mathcal{H}_\infty$ controller to arrive at a robustly performing control design. Experiments were conducted on the physical system, verifying the robustness of the controller.**

I. Introduction

The inverted pendulum is a classic problem in control systems, characterized by its stable and unstable equilibria. A myriad of control design techniques have been applied to stabilize the inverted pendulum, with some control schemes even able to swing the pendulum up to its inverted state. Because the inverted pendulum is such a canonical example of a nonlinear dynamic system, we can often gain insight into controlling other nonlinear systems by attemping to control the pendulum.

The control design presented here considers the problem of regulation of the pendulum to the origin. In other words, the objective is to balance the inverted pendulum on the cart, while keeping it in the center of the track and rejecting exogenous disturbances. In considering a robust control design for the system, it is necessary to identify uncertainties and sources of disturbances. The stability analysis and control design applied here applies to a very specific system manufactured for educational purposes by Quanser, pictured in Figure 1.

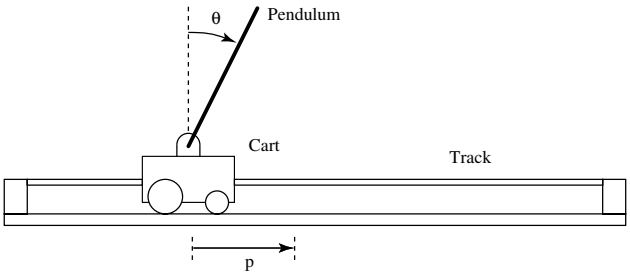

Fig. 1. Inverted Pendulum System

The cart is actuated by a DC motor. The DC motor applies torque to a pinion, which moves the cart across a rack mounted on the track. The pendulum is mounted to a free-spinning shaft, with negligible friction. Measurements are provided by two encoders, which measure cart position and angular displacement of the encoder shaft. The measurements and control signals are routed through a Quanser digital interface board which performs quadrature decoding of the encoder signals and digital to analog conversion of the voltage signal going to the motor. In the D/A conversion, a hard ± 5V limit is imposed on the control signal, inducing an ideal saturation. Distrubances in the system are due to external forces applied to the cart or pendulum and measurement noise created from encoder quantization.

The remainder of this paper explores this problem in detail and is organized as follows. Section II breifly describes the cart-pendulum system and a corresponding dynamic model. Section III addresses uncertainty in the dynamic model and presents a perturbation structure for the system. Section IV presents a nominal H_∞ design and refines this design through D-K iteration. A frequency dependent μ calculation is performed at each iteration to analyze robust performance and stability. Section V presents experimental results using the designed controller on the Quanser apparatus.

II. Dynamic Model

The cart-pendulum apparatus is a simple mechanical system, in which the equations of motion can be derived by applying Newton's laws of motion to the free body diagram, pictured in Figure 2.

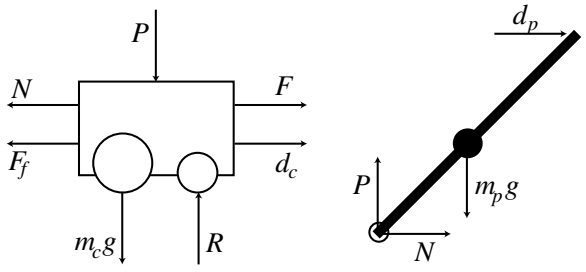

Fig. 2. Inverted Pendulum Free Body Diagram

The control input to the system is a voltage applied to the motor, generating the force, F, on the cart. It is worth noting that in the model, the DC motor is assumed to produce an instantaneous torque, given in (1). Disturbances to the system are assumed to enter as a force on the cart, d_c, or as a force on the pendulum, d_p. Additionally, P and N represent the equal and opposite interaction of forces between the cart and pendulum, while R is the restoring force from the track and

F_f represents viscous friction incurred from the cart sliding along the track.

In addition to the terms present as forces, there are several physical constants associated with the system that must be defined. These are presented in Table I.

Parameter	Symbol
Motor Torque Constant	K_m
Gear-box Ratio	K_g
Motor Armature Resistance	R
Motor Pinioin Radius	r
Cart Mass	m_c
Pendulum Mass	m_p
Rotational Inertia	I
Half-Length of Pendulum	l

TABLE I

QUANSER CART-PENDULUM SYSTEM PARAMETERS

For the sake of brevity, we define two additional terms, $M = m_c + m_p$ and $L = \frac{I+m_p l^2}{m_p l}$. As previously mentioned, the force generated by the DC motor depends on both the voltage applied to the motor, V, and the velocity of the cart, $\dot{p}$, and is given by

$$F = \frac{K_m K_g}{Rr} V - \frac{K_m^2 K_g^2}{Rr^2} \dot{p}. \tag{1}$$

Since the dynamic equation derivation is not the focus of this paper, the equations are only *displayed* in (2) and (3). For the interested reader, the dynamic equations are derived in great detail in [1] (without the inclusion of disturbances or an extra frictioinal term).

$$\begin{aligned} \ddot{p} \;=\; & \frac{1}{(M - \frac{m_p l \cos^2(\theta)}{L})} \Bigg(F - b\dot{p} - \frac{m_p l g \cos(\theta)\sin(\theta)}{L} \\ & + m_p l \sin(\theta)\dot{\theta}^2 \\ & - \left(1 + 2l\frac{\cos(\theta)}{I + m_p l^2}\right) d_p + d_c \Bigg) \end{aligned} \tag{2}$$

$$\begin{aligned} \ddot{\theta} \;=\; & \frac{1}{(L - \frac{m_p l \cos^2(\theta)}{M})} \Bigg(g\sin(\theta) - \frac{m_p l \cos(\theta)\sin(\theta)\dot{\theta}^2}{M} \\ & + \frac{\cos(\theta)}{M} \left(b\dot{p} - F - d_c + \left(\frac{1}{M} + \frac{2}{m_p}\right) d_p \right) \Bigg) \end{aligned} \tag{3}$$

Since we are employing a linear control design in this paper, a linear state space resentation is extracted from (2) and (3) in the following manner. State, input, and output vectors are defined as

$$\begin{bmatrix} x_1 & x_2 & x_3 & x_4 \end{bmatrix}^\top = \begin{bmatrix} p & \dot{p} & \theta & \dot{\theta} \end{bmatrix},$$
$$\begin{bmatrix} u_1 & u_2 & u_3 \end{bmatrix}^\top = \begin{bmatrix} d_c & d_p & V \end{bmatrix},$$

and

$$\begin{bmatrix} y_1 & y_2 \end{bmatrix}^\top = \begin{bmatrix} p & \theta \end{bmatrix},$$

respectively. A linearization of (2) and (3) is then taken about the equilbrium, $x_e = \begin{bmatrix} 0 & 0 & 0 & 0 \end{bmatrix}^\top$ and $u_e = \begin{bmatrix} 0 & 0 & 0 \end{bmatrix}^\top$. In this paper, a digital controller is desired, so a zero-order-hold equivalence is taken of the resulting linearization, with a sampling period of $T_s = 0.0005$s. The associated frequency responses of the nominal model are shown in Figure 3. It is worth noting that the affect of both disturbances on the angle are the same and their Bode plots are overlayed.

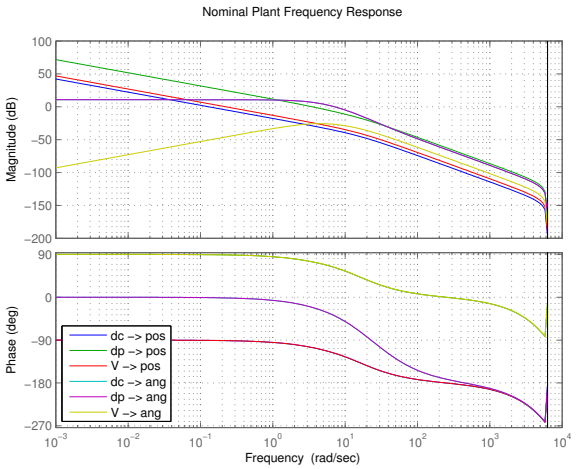

Fig. 3. Frequency Response of Nominal Model

Note that the frequency response from V to p and from V to θ differ greatly. While the response from V to p is essentially an integrator, the response from V to θ is somewhat of a band-pass filter. This will play a role in the amount of performance we can ask from the system over certain frequency ranges in Section IV-A.

III. PERTURBATION MODEL

In this paper, we wish to stabilize the set of systems generated by uncertainty in parameters. The measured values of the parameters are given by the Quanser lab manual; however, some of these parameters, shown in Table I, can vary with time, and others may be difficult to measure. In the proceeding analysis, variations in the motor torque constant, motor armature resistance, cart mass, and pendulum mass (and the resulting pendulum inertia) will be considered, as well as an additional frictional term not present in the nominal model provided by Quanser.

The aforementioned terms are assumed to have a 15% relative uncertainty, with the exception of the frictional term, b, assumed to vary between 0 (nominal) and $1\frac{\text{N}}{\text{m/s}}$. The maximum value of b is about 10% of the maximum force expected to be generated by the DC motor.

For our purposes, we choose to use a single, input multiplicative perturbation in hopes of capturing the model variation. In the following calculation, we assume that the effect of the input multiplicative perturbation is the same as an

output multiplicative perturbation on each output, allowing us to extract an upper bound on the perturbation magnitude.

In order to derive a perturbation weight for the system, these assumptions are used in a Monte Carlo analysis of the set of possible dynamic models. Through each trial performed, the frequency response of the dynamic model is caluclated using values from the uncertain parameter space mentioned previously (they are selected from a uniform distribution). With each of these frequency response calculations, a multiplicative perturbation is calculated according to (4),

$$\Delta_{m,i}(z) = \frac{P_i(z) - P_{nom}(z)}{P_{nom}(z)}, \tag{4}$$

where $P_i(z)$ refers to the i-th randomized model transfer function, from V to p (by our assumptions, we only need look at one transfer function) and $P_{nom}(z)$ refers to the nominal model (calculated from the nomial values given by Quanser). Observing the frequency responses of $\{P_i(z)\}$, we then fit a multiplicative uncertainity bound, $W_m(z)$, over the set of all calculated $\Delta_{m,i}$. This is shown in Figure 4. The perturbation bound, $W_m(z)$, is chosen as

$$W_m(z) = \frac{1.119z - 1.116}{z - 0.9844}. \tag{5}$$

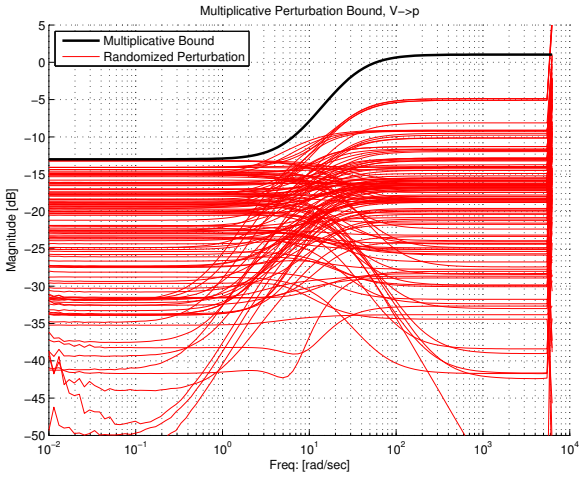

Fig. 4. A Multiplicative Perturbation Bound

Examining Figure 4, we see that our nominal model is believable for low frequencies; however, as frequency increases, the integrity of the nominal model decays. Note also that W_m is chosen to cross 0dB around 10Hz. This will provide enough useful bandwidth for the controller to act within while rolling off high frequencies where the nominal model is functionally unknown.

For the subsequent μ analysis of robust stability, the perturbation block structure will be

$$\mathbf{\Delta} = \{\Delta | \Delta \in \mathbb{C}^{1\times 1}\}. \tag{6}$$

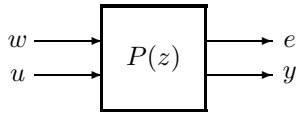

Fig. 5. Representation of Plant for $\mathcal{H}_\infty$ Design

IV. Robust Control Design

The control design process presented here consists of two main components. The first is a nominal $\mathcal{H}_\infty$ design, where appropriate pentalties and performance expectations are applied to the plant. The `hinfsyn()` function in MATLAB is then used to calculate the controller. The second design component is D-K iteration, where the nominal controller is used as a foundation to compute a robustly performing controller.

Before testing the design on the Quanser apparatus, a hi-fidelity simulation is conducted, which utilizes the nonlinear ODE's describing the system, measurement noise present from encoder sensors, saturation effects resulting from digital to analog conversion, and outside disturbances to the pendulum and cart. Despite its detail, the simulation is ultimately driven by the ODE's, which rely on the nominal values of the system parameters given by Quanser. Hence, the simulation can only provide information about performance and stability in the nominal case. To achieve the desired performance on the set of all perturbed models, we will rely on D-K iteration.

A. $\mathcal{H}_\infty$ Design

Since the controller synthesis is performed for us by MATLAB, the design problem is reduced to organizing the problem for MATLAB to interpret and choosing frequency dependent penalties and weights for the relevant signals. Figure 5 displays the representation of the plant needed to use `hinfsyn()`, where e denotes the vector of controlled error signals, w denotes the vector of exogenous inputs, y is the vector of measurements, and u is the vector of control inputs. Table II summarizes the content of these vectors, and for each weighted signal, shows the name of the frequency domain weight, depicted in Figure 6.

Signal Vector	Content	Weight Name
w	Cart Disturbance	Wdc
	Pendulum Disturbance	Wdp
	Position Measurement Noise	$Wdmc$
	Angle Measurement Noise	$Wdmp$
u	Voltage Input	- -
e	Position Error (from origin)	$Wpos$
	Angle Error (from origin)	$Wang$
	Actuator Penalty	Wv
y	Position Measurement	- -
	Pendulum Angle Measurement	- -

TABLE II
SIGNALS IN PLANT MODEL FOR $\mathcal{H}_\infty$ DESIGN

To tailor the design towards our pendulum system, weights are applied to each signal in w and e, either applying a penalty

to an error signal, or shaping an exogenous input. The weights are shown in Figure 6, corresponding to the signals in Table II. In addition, Figure 6 also shows the multiplicative perturbation bound for comparison.

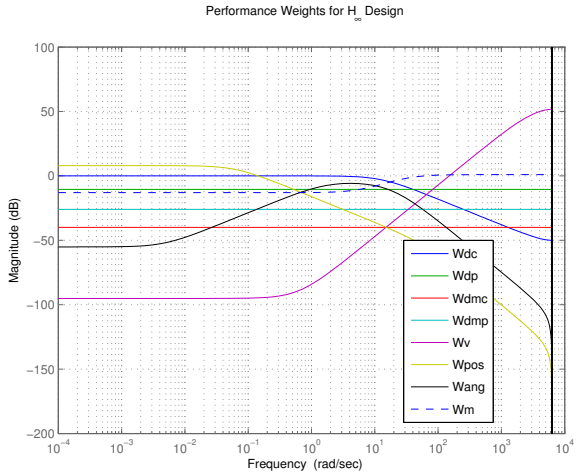

Fig. 6. $\mathcal{H}_\infty$ Design Penalties

The type of disturbances expected for the cart and pendulum, d_c and d_p, respectively, are pulses. The pendulum disturbance is modeled as an impulse (hence the flat weight), while the cart disturbance is expected to be a short pulse, greater in amplitude than the pendulum disturbance. The measurement noise is assumed to have a constant frequency spectrum, with the angle measurement noise larger in magnitude than the position measurement noise.

The actuator penalty, Wv, asks for only low frequency signals, in hopes of attenuating the effects of measurement noise on on the control signal. Note now, that $Wpos$ asks for performance only at low frequencies. This is natural to ask for, as these frequencies are easily expressed through the response from V to p shown in Figure 3. Lastly, $Wang$ asks for performance only in mid range frequencies, as these are most easily expressed by the nominal plant. In comparison with the perturbation weight, each of the performance expectations does not ask for performance past the point where the model integrity begins to degrade. This is done intentionally, as it doesn't make sense to ask for performance where the plant is unknown.

Figure 7 shows simulation results, in which the $\mathcal{H}_\infty$ controller rejects a rather adverse disturbance to the cart and pendulum. It is worth noting that the scale on the control signal is in 25V increments, so each increment of 0.05 on the plot corresponds to an increment of 1.25V and a value of 0.2 corresponds to 5V (the saturation limit). In this simulation, most of the available control effort has been exhausted. While the nominal design seems to perform well, it is worth emphasizing again that the simulation uses the nominal parameter values given by Quanser.

As might be expected, Figure 8 shows a μ calculation of the unweighted closed loop, where it is clear that the nominal

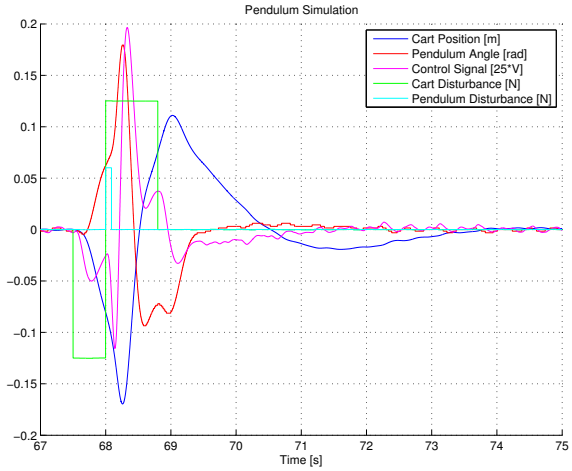

Fig. 7. $\mathcal{H}_\infty$ Design Simulation

design is not robustly stable. Indeed, the value of μ spikes as the nominal model begins to degrade.

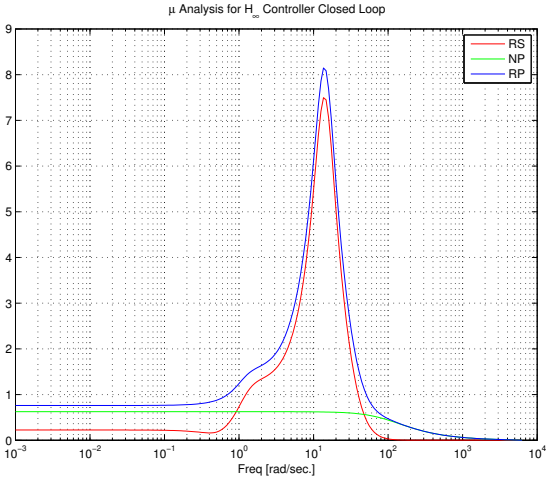

Fig. 8. $\mathcal{H}_\infty$ Design μ Caclulation

B. D-K Iteration

Since the $\mathcal{H}_\infty$ design is not robustly stabilizing (even less, robustly performing), D-K iteration is employed to improve the stability in the destabilizing frequency ranges. Through each iteration, the D-scale matrix is extracted from the μ calculation and approximated by a filter. The order of the filter is selected so that the approximation accurately reflects the value of μ over the crictical frequency ranges. An example of this fitting procedure is provided in Figure 9.

Here we can see that a constant fit ($n = 0$) does not accurately reflect the value of μ. In this iteration, a 2^{nd} order fit is selected, as it does not exaggerate the value of μ in critical areas while maintaining a close fit in other frequency ranges. Here, it might be possible to select a 1^{st} order fit, but a tight fit around the peak close to $2\frac{\text{rad}}{\text{s}}$ is desired.

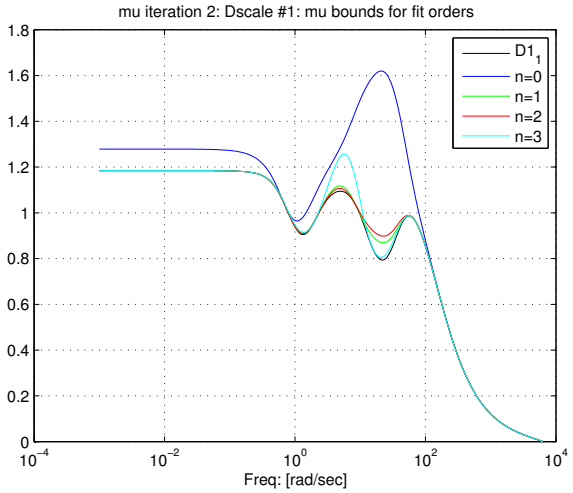

Fig. 9. Example D-Scale Fitting

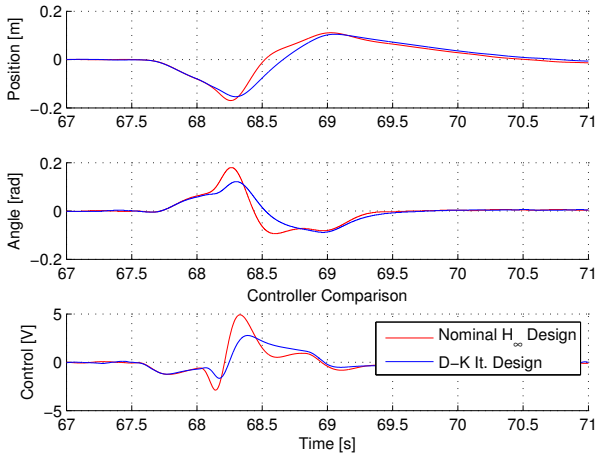

Fig. 11. Closed Loop Response Comparison (Simulation)

Once the D-scale is approximated, the plant is scaled appropriately and an $\mathcal{H}_\infty$ design is synthesized for the scaled plant. This procedure is repeated until (hopefully), the μ calculation for robust performance yields a value less than 1 for all frequencies. When applied to our inverted pendulum system, 3 full iterations result in a design that performs robustly. Figure 10 shows the evolution of the frequency dependent robust performance measure through each iteration. Note that even a single iteration yields a significant difference with the nominal design (compare with Figure 8).

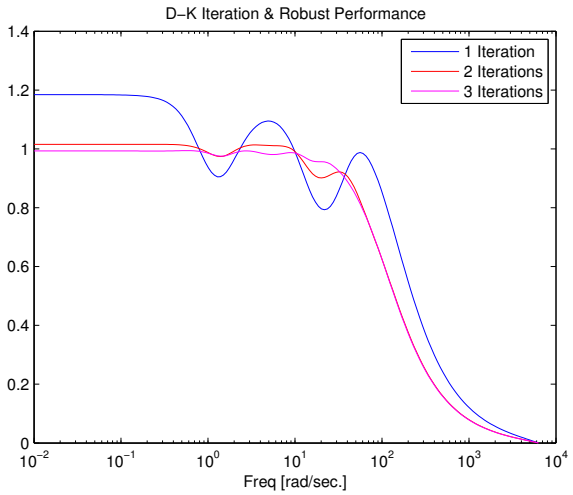

Fig. 10. Robust Performance Evolution Through D-K Iteration

With the D-K iteration complete, we can compare the nominal design with the iterative design. Figure 11 shows the simulated response of the closed loop systems to the same disturbances as in Figure 7.

Here, we can see that when controlling the nominal model, the controller resulting from D-K iteration seems to have a milder response. The error signals behave in a less erradic fashion and do not seem to peak as high as when using the nominal design. This is somewhat unexpected, as designing for a *robustly* performing controller usually entails the sacrifice of *nominal* performance.

V. Experimental Results

Implementing control design on any physical system involves some *leap of faith*. In this setting, we have attempted to design for a set of dynamic models of the system, compensating for 15% relative uncertainty in several system parameters. In implementing the controller on the physical system, we hope that it is adequately described by our model set.

While several experiments were conducted on the system, only one is presented here. Not surprisingly, the nominal $\mathcal{H}_\infty$ controller actually *failed* to stabilize the system, so the experiment shown used the controller designed by D-K iteration. In each experiment, the system began at the origin and disturbances were introduced as time progressed. The experiment shown tested the controller on the cart system, with extra weights attached to the cart and to the middle of the pendulum. The pendulum weight was attached to the middle for reasons explained later. Table III summarizes the weight characteristics used in the experiment. Note that in Table III, the measured cart mass already had a 15% relative difference with the nominal value. Also note the *large* amount of weight added to the cart and pendulum. Certainly, the stability and performance seen in the experiment was not guaranteed by the μ analysis. Needless to say, stability and performance without the added weight was better than with the weights.

Figure 12 shows the result of the weighted experiment. During the experiment, the pendulum was subjected to a distubance around 5s and the cart was subjected to a disturbance around 10s. While these disturbance-driven experiments are not repeatable, they still adequately verify performance results for the closed-loop system. In each experiment, the system seemed to oscillate about the origin when undisturbed. This is somewhat apparent in the data shown, as the cart and

Object	Mass (g)	Extra Mass (g)	(%) Difference
Cart (nom.)	455	- -	- -
Pendulum (nom.)	210	- -	- -
Cart (meas.)	521	323	85
Pendulum (meas.)	210	575	274

TABLE III
MASSES ON CART-PENDULUM SYSTEM

pendulum do not return to the origin after the disturbance. Another shortcoming of the controller was the control effort needed to stabilize the system. In the experiment shown, the control signal spiked above 5V, saturating the actuator and possibly inducing windup.

Despite its shortcomings, the controller seemed to perform well, especially in comparison with the failure of the nominal controller. After all, it managed to stabilize the system with and without large weights *and* in the presence of quite adverse disturbances and measurement noise.

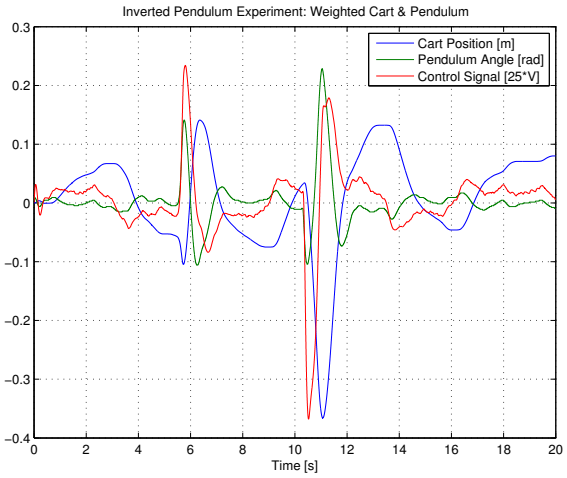

Fig. 12. Inverted Pendulum Experiment: Cart & Pendulum Weighted

Other experiments conducted involved changing the amount or position of the pendulum and cart masses. During the experiment shown in Figure 12, the pendulum weight was placed in the middle, at half the height of the pendulum. At this position, the controller performance did not seem substantially worse, despite the extra weight. However, positioning the weight at the top of the pendulum resulted in *substantially* worse performance. When subjected to small disturbances, the system would oscillate for several seconds before coming to a rest. This can be explained by the very large difference in rotational intertia caused by placing the weight at the top of the pendulum.

VI. CONCLUDING REMARKS

In this paper, we set out to design a robustly performing controller for an inverted pendulum on a motorized cart. Through a Monte Carlo analysis of the model's frequency response, a perturbation model was established. Using MATLAB, an $\mathcal{H}_\infty$ controller for the nominal system was synthesized which did not perform robustly. To remedy this, D-K iteration was employed to compute a controller that yielded the desired robust performance. Each control design was tested on the actual system, where the nominal $\mathcal{H}_\infty$ design failed to stabilize the pendulum, but the controller computed from D-K iteration succeeded.

In essence, the results presented in this paper constitute an excellent example of Robust Control theory. When the nominal controller was synthesized, it was found not to be robustly stable. Hence, there was no surprise when it failed to stabilize the physical system. In the language of Robust Control, the actual system differed from the nominal model by a perturbation which was destabilizing for the nominal controller. After performing D-K iteration, we arrived at a robustly stable controller (via a μ calculation), which managed to stabilize the actual system. In essence, the variation of the physical system about the model was captured by our perturbation model and compensated for by our robustly stable controller.

While the performance of the actual system suffered from a couple shortcomings, it could be improved thorugh re-design. Possibly, to eliminate the excessive oscillation about the origin, one could re-design the weights used for the nominal design, in hopes that those characteristics would carry through the D-K iteration. Expanding the bandwidth of the position performance weight might help, as in this design, it is very small. The low frequency oscillations present in the position may be manifesting themselves because this frequency is easily expressed through the plant, but not penalized by the controller. The same may be true of the pendulum angle. Expanding the performance weight bandwidth towards lower frequencies may help eliminate this problem.

While these suggestions may help the actual performance, it is difficult to predict the extent to which their impact on the nominal design will transcend the D-K iteration. Also, expecting more performance out of the system may push the value of μ too high. As always, there is some tradeoff to be made.

REFERENCES

[1] R. Smith, *ECE147b: Digital Control. Lab 3: Balancing the Inverted Pendulum*, `http://www-ccec.ece.ucsb.edu/people/smith/`